Three-polarizer Treatment of Linear Polarization in Coronagraphs and Heliospheric Imagers

Craig E. DeForest , Daniel B. Seaton , and Matthew J. West
Southwest Research Institute, 1050 Walnut Street, Suite 300, Boulder, CO 80302, USA; deforest@boulder.swri.edu

Abstract

Linearly polarized light has been used to view the solar corona for over 150 years. While the familiar Stokes representation for polarimetry is complete, it is best matched to a laboratory setting and therefore is not the most convenient representation either for coronal instrument design or for coronal data analysis. Over the last 100 years of development of coronagraphs and heliospheric imagers, various representations have been used for both direct measurement and analysis. These systems include famous representations such as the (B, pB) system, which is analogous to the Stokes system in solar observing coordinates, and also internal representations such as in-instrument Stokes parameters with fixed or variable "vertical" direction, and brightness values through a particular polarizing optic or set thereof. Many polarimetric instruments currently use a symmetric three-polarizer measurement and representation system (which we refer to as "(M, Z, P)") to derive the (B, pB) or Stokes parameters. We present a symmetric derivation of (B, pB) and Stokes parameters from (M, Z, P), analyze the noise properties of (M, Z, P) in the context of instrument design, develop (M, Z, P) as a useful intermediate system for data analysis including background subtraction, and draw a helpful analogy between linear polarimetric systems and the large existing body of work on photometric colorimetry.

Unified Astronomy Thesaurus concepts: Polarimetry (1278); Solar K corona (2042); Color equation (269); Polarimeters (1277); Solar instruments (1499)

1. Introduction

The solar corona is linearly polarized (Arago 1843). That property has been exploited over nearly a century of coronal observations: both for background removal in coronagraphs (Lyot 1930) and for 3D analysis (Poland & Munro 1976; de Koning & Pizzo 2011; DeForest et al. 2017).

The degree of coronal polarization is conventionally reported via two parameters: a B ("unpolarized brightness") parameter and its counterpart pB ("polarized brightness"); and both parameters may be mapped over an image plane to create separate "B images" and "pB images." Because the corona is a distributed object, it is best tracked via its radiance (delivered optical power per unit area, per unit solid angle), and therefore "brightness" and "radiance" are synonyms. The K corona is visible primarily via Thomson scattering and therefore it is polarized perpendicular to the plane containing the observer, the Sun, and the scattering point. At each point in a two-dimensional image plane, the K corona is thus polarized perpendicular to a line extending through the imaged center of the Sun and the given point (Figure 1(a)); this direction is not only predicted by theory (e.g., Billings 1966; Howard & Tappin 2009) but also readily verified through direct measurement (e.g., Filippov et al. 1994). pB may thus be calculated as

$$pB = B_T - B_R, \qquad (1)$$

where B_T is the radiance observed through a linear polarizer oriented tangentially to a solar-concentric circle passing through the image point of interest, and B_R is the radiance observed through a linear polarizer oriented radially to the Sun

through the same point (e.g., Minnaert 1930; Altschuler & Perry 1972). Whether Equation (1) is accidental or fundamental to the definition of pB is a matter of ongoing historical confusion and even dispute. This is explored in an Appendix to this article, which introduces a $^{\circ}pB$ and $^{\perp}pB$ to distinguish historical usage. In this work we treat Equation (1) as fundamental; this treatment implies that pB is similar to the Stokes Q parameter (e.g., Hecht & Zajac 1974), but in a coordinate system that is rotated relative to the instrument.

The (B, pB) representation of coronal polarization is convenient because it matches the observing geometry, and in fact many coronagraphs have been constructed to measure directly that element of linear polarization (e.g., Altschuler & Perry 1972). However, because the direction of "radial" varies in the image plane, this adds complexity to the instrument itself. Recent spaceborne coronagraphs have instead measured the full linear polarization state of incident light in the instrument frame (e.g., Brueckner et al. 1995; Howard et al. 2008). This requires capturing the first three Stokes parameters (I, Q, U) at each location of the image plane, either directly or indirectly via a representative measurement.

The Stokes (I, Q, U) parameters are defined in terms of exposures through individual crossed polarizers in a laboratory, and the textbook approach to measurement involves four exposures through crossed polarizers in the fixed instrument reference frame: horizontal/vertical for Q and diagonal for U (Figure 1(b); Hecht & Zajac 1974). However, only three independent measurements are necessary to determine the linear polarization states of a beam of light. This was the basis of the triplet polarizing camera used by Öhman (1947) to observe the 1945 eclipse, and Öhman attributed the technique to an earlier analysis by Fesenkov (1935). The technique is described briefly in Chapter 4 of Billings (1966) and by Newkirk et al. (1970); these authors both used the Stokes
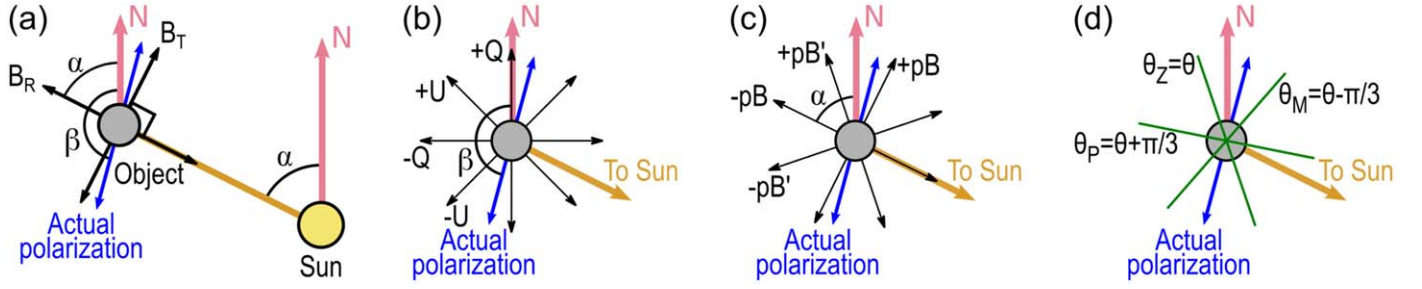
Figure 1. Four panels describe linear polarization analysis in a coronal context. (a) An object near the Sun has position angle α and polarization angle β; B_R and B_T describe brightnesses through radially and tangentially aligned polarizers. (b) Stokes Q and U describe polarization in the "+" and "×" directions relative to the instrument (or solar north). (c) pB and pB' are Stokes parameter analogs in the solar observing reference frame. (d) Observing polarization through three polarizers mutually separated by $\pi/3$ radians is sufficient to capture the polarization state (I, Q, U) or, equivalently, (B, pB, pB'). Although Thomson-scattered light is polarized in the B_T direction, we show the polarization vector slightly misaligned, to emphasize the general case.

parameters as an intermediary system, rather than treating the triplet analysis as primary. Polarization triplet analysis has been and is still used routinely with coronal images from Skylab (Poland & Munro 1976), SOHO/LASCO (Brueckner et al. 1995), and STEREO/SECCHI (Howard et al. 2008), and is planned for other instruments in development.

Despite its common use, full descriptions of the polarizer triplet technique, including instrumental effects, are elusive in the current literature; and those that exist are somewhat unsatisfying because, in translating through the Stokes system, the analytic work loses the symmetry of the polarizer triplet system. In this article, we derive formulae to find directly the (B, pB, pB') or Stokes (I, Q, U) representations of linear polarization from polarizer triplet data; present an analytic noise analysis for the most likely sources of noise or systematic error in a real instrument using a polarizer triplet; introduce the use of an (M, Z, P) system of "virtual polarizer triplets" (Figure 1(d)) to represent the linear polarization state of light in frames other than the observing frame; and draw a surprising but helpful analogy between the major systems of linear polarimetry and corresponding systems for representing color.

2. Definitions

Table 1 defines several quantities, including radiances, polarization parameters, and angles, that are relevant to a polarizing coronagraph or heliospheric imager. These quantities are used throughout Section 3, and are collected here for reference. Figure 1 illustrates the angles and associated angles of the principal quantities in Table 1.

3. Linear Polarization from Three Polarizers

We start by deriving a formula for pB and B at position angle α, with coronal light polarized along the direction $\alpha + \pi/2$. This further leads to expressions for extracting the direction of polarization, and the full linear portion of the Stokes representation. Since α is the angle of a radial line, the polarization direction β is just $\alpha + \pi/2$ (tangential) for Thomson-scattered light in the corona.

Solving the definitional expressions for B and pB in Table 1, for B_T and B_R we have

$$B_T = \frac{B + pB}{2} \quad \text{and} \quad B_R = \frac{B - pB}{2}. \tag{2}$$

Admitting the light through a polarizer at angle θ projects the electric field to the new direction; intensity is the square of the

Table 1
Useful Quantities in a Linear Polarimetric Coronagraph

Quantity	Expression	Definition
$B_{\{T,R\}}$	⋯	Radiance via an ideal polarizer oriented tangentially or radially relative to the Sun
B	$B_T + B_R$	"Unpolarized brightness" (radiance)
pB	$B_T - B_R$	Coronal "polarized brightness"
α	⋯	Solar position angle of an image point
β	⋯	Direction of polarization
θ	⋯	Polarizer angle (also subscripted as θ_i)
θ_i	$\theta + \{-1, 0, 1\}\pi/3$	One of three angles in an (M, Z, P) triplet
ϕ	⋯	Second polarizer angle
B_θ	⋯	Radiance through a polarizer at angle θ
B_i	⋯	Radiance through a polarizer at angle θ_i
$B_{\{\|,-,/,\backslash\}}$	⋯	Radiance through an ideal polarizer oriented at $n\pi/4$ ($n \in \mathbb{Z}$)
I	$B_\| + B_-$ $B_\backslash + B_/$	Stokes I—synonym for B (sum of radiance through any two perpendicular polarizers)
Q	$B_\| - B_-$	Stokes Q (in instrument frame)
U	$B_\backslash - B_/$	Stokes U (in instrument frame)
p	$\sqrt{Q^2 + U^2}\big/I$	Polarization fraction (note: for Thomson scattering, $pB = (p)(B)$)
S_i	$\sin[2(\theta_i - \alpha)]$	Convenient abbreviation for sine expression
C_i	$\cos[2(\theta_i - \alpha)]$	Convenient abbreviation for cosine expression

Note. In this context, Stokes I is a radiance, not an intensity. Lists in curly braces enumerate options for the relevant expression.

electric field amplitude, so

$$B_\theta = B_T[\sin(\theta - \alpha)]^2 + B_R[\cos(\theta - \alpha)]^2. \tag{3}$$

Substituting and applying the double-angle cosine formula,

$$B_\theta = \frac{1}{2}\{B - pB\cos[2(\theta - \alpha)]\}, \tag{4}$$

which is the projection equation for partially polarized light. Solving for pB in terms of B and B_θ yields:

$$pB = \frac{B - 2B_\theta}{\cos[2(\theta - \alpha)]}, \qquad (5)$$

which resolves pB in terms of the radiance through a single arbitrary polarizer and also the total radiance with no polarizers in the beam. Equation (5) is problematic, because the denominator is small when $\theta - \alpha$ is near $\pm\pi/4$. If multiple polarizers are available at different angles, one can regularize Equation (5) by taking an average and weighting each term by the square of the offending cosine. Adopting the C_i abbreviation (Table 1),

$$pB = \frac{\sum_i \{(B - 2B_i)C_i\}}{\sum_i C_i^2} \qquad (6)$$

which is numerically stable if the θ_i are not all separated by intervals of $n\pi/2$. Choosing the (M, Z, P)[1] basis of polarizers at $\theta - \pi/3$, θ, and $\theta + \pi/3$, the denominator sum evaluates to $3/2$ and the B terms sum to zero, so

$$pB = -\frac{4}{3} \sum_{i \in \{M,Z,P\}} (B_i C_i) \qquad (7)$$

Meanwhile, solving Equation (4) for B yields

$$B = 2B_\theta + C\, pB, \qquad (8)$$

where C is not subscripted because here it appears outside a sum. Equation (8) is not particularly useful by itself—but averaging over the three polarizer positions of the (M, Z, P) system eliminates the cosine through a trigonometric identity, yielding

$$B = \frac{2}{3} \sum_{i \in \{M,Z,P\}} B_i. \qquad (9)$$

Equations (7) and (9) give B and pB in closed and symmetrical form, given radiance data through three polarizers with relative angles of $-\pi/3$, 0, and $+\pi/3$ radians (60° separation) relative to a baseline angle θ, with the assumption that the direction of linear polarization is perpendicular to α.

Note that, although α is defined (in Table 1) as position angle around the Sun, nothing in Equations (7) and (9) requires any particular value of α—or, for that matter, any particular orientation of the main polarization direction θ. In fact, in the special case where $\alpha = \pi/2$, B and pB are just the Stokes I and Q parameters in the solar reference frame. Working by analogy to the Stokes parameters, we can substitute $\alpha \rightarrow \alpha + \pi/4$ into Equation (7); this yields a similar quantity that reduces to Stokes U in the same circumstance:

$$pB' = -\frac{4}{3} \sum_{i \in \{M,Z,P\}} (B_i S_i) \qquad (10)$$

where the new quantity pB' bears the same relationship to pB as Stokes U does to Stokes Q. In systems where pB' is important, we must generalize Equation (4) to include pB':

$$B_\theta = \frac{1}{2}\{B - C\, pB - S\, pB'\} \qquad (11)$$

where the difference between Equations (4) and (11) is that the former assumes tangential polarization while the latter treats arbitrary linear polarization. Repeating the derivation of Equation (7) using Equation (11) instead of (4) yields the same result, because the C_i-weighted summation in Equation (7) eliminates the $S_i\, pB'$ terms from Equation (11).

The B, pB, pB' system is an analog of the Stokes I, Q, U system, but rotates with α around the Sun rather than being fixed in the instrument frame of reference; the familiar Stokes parameters may be recovered by substituting $\alpha = \pi/2$ into Equations (7), (9), and (10). In the special case where the polarizer triplet is aligned with the instrument, one may also set $\theta = 0$ and arrive, after many cancellations, at the simplified expressions

$$Q = \frac{2}{3}(2B_Z - B_M - B_P) \qquad (12)$$

and

$$U = \frac{2}{\sqrt{3}}(B_P - B_M), \qquad (13)$$

which (together with the identity $B = I$) define the Stokes I, Q, U triplet relative to the reference Z polarizer in the M, Z, P system, with a minimum of calculation. Equations (12) and (13) reproduce the derivations presented by Öhman (1947) and Billings (1966).

The remaining important system to represent linear polarization is (B, θ, p), which uses the overall brightness B, direction of polarization θ, and normalized degree of polarization p. The direction of polarization is available from pB and pB' (or, equivalently, from Stokes Q and U). Differentiating Equation (11) to find the maximum value of B_θ,

$$\left.\frac{\partial B_\theta}{\partial \theta}\right|_{\theta = \theta_{max}} = S\, pB - C\, pB' = 0, \qquad (14)$$

so

$$\theta_{max} = \frac{1}{2} \arctan\left(\frac{pB'}{pB}\right) + \frac{\pi}{2} + \alpha, \qquad (15)$$

where the four-quadrant arctan is implied and selects maxima rather than minima, and the $\pi/2$ arises from canceling negative signs in the numerator and denominator of the arctan (adding π to the result of the four-quadrant arctan). Making use of Equation (15), substituting the arctan into Equation (11), and recognizing two trigonometric cancellations yields the expected formula for p:

$$p \equiv \frac{2B_{\theta,max} - B}{B} = \frac{\sqrt{pB^2 + pB'^2}}{B}. \qquad (16)$$

Equations (15) and (16) recover the textbook formulae for θ and p from the Stokes formalism, in the context of the (B, pB, pB') system instead of (I, Q, U).

3.1. Error Sources in Three-polarizer Polarimetry

Polarimetry is affected by multiple error and noise sources that are specific to the measurement. Here we derive expressions for calculating the error or noise associated with three-polarizer measurements of B and pB, given important photometric or mechanical tolerances of the instrument. The three major potential

---

[1] For "Minus, Zero, Plus".

sources of error are photometric noise, polarizer misalignment errors, and finite polarizer effectiveness. We consider noise as an approximately Gaussian-distributed random variable, with mean value of zero, added to the true value of each quantity.

To keep track of which quantities represent physical truth (with no noise nor measurement error) and which represent inference from measurement (with noise and other error sources included), we introduce an overbar to indicate directly or indirectly measured parameters:

$$\bar{X} \equiv X + \Delta X, \tag{17}$$

where X is an observable parameter such as B or pB, $\bar{X}$ is the observed value, and ΔX is a noise term.

Furthermore, we take the indices i and j to run over the (M, Z, P) polarizer angles when mentioned in a summation, in keeping with Equations (7), (9), and (10).

3.1.1. Photometric Errors

Propagating photometric error and noise through measurements from multiple polarizers is straightforward. Photometry is most frequently limited by Poisson-distributed photon shot noise or similar uncorrelated noise sources. Systematic errors can also contribute to total error; we neglect these terms, which is equivalent to treating systematics in each channel as randomly distributed across channels. To each value B_i we add a noise term ΔB_i that we treat as a sample of a random variable. To propagate noise from the three samples, we take the partial derivative of Equations (7), (9), and (10) with respect to an arbitrary polarizer brightness, then sum the ΔB_i terms in quadrature. This approach works because Equations (7), (9), and (10) are linear in B_i; and also the B_i noise samples are taken to be uncorrelated. Equation (9) is straightforward to differentiate:

$$\frac{\partial \bar{B}}{\partial \bar{B}_i} = \frac{2}{3}. \tag{18}$$

In the most common case for image detectors, there is both a signal-independent noise component and a Poisson-statistics photon counting noise component, adding in quadrature. In that case, we have

$$\Delta B_i = \sqrt{(\Delta_c B)^2 + B_0 B_i}, \tag{19}$$

where $\Delta_c B$ is the signal-independent noise term (such as detector dark noise or read noise), B_0 is an instrument-specific constant of proportionality relating radiance units to detection quanta at an individual pixel or detector, and $\sqrt{B_0 B_i}$ is the Poisson noise term that arises from counting statistics. Merging the noise terms explicitly using Equation (9) and quadrature summation yields

$$\Delta B = \frac{2}{3} \sqrt{\sum_i [(\Delta_c B)^2 + B_0 B_i]}, \tag{20}$$

or, substituting from Equation (11),

$$\Delta B = \frac{2}{3} \sqrt{3(\Delta_c B)^2 + \frac{B_0}{2} \sum_i (B - C_i pB - S_i pB')}. \tag{21}$$

The C_i terms and the S_i terms sum to zero, leaving

$$\Delta B = \frac{2}{\sqrt{3}} \sqrt{(\Delta_c B)^2 + B_0 B/2}, \tag{22}$$

which, in the special case of unpolarized light (so that $B_i = B/2$ for each i), would reduce, for each i, to

$$\Delta B = \frac{2}{\sqrt{3}} \Delta B_i, \tag{23}$$

which arises from Equation (22) by substituting B_i for $B/2$ and noticing that the sum matches the right-hand side of Equation (19).

Because Equation (22) is independent of pB and pB' for polarizer triplets, the photometric ΔB may be calculated for the unpolarized case and remains valid in the polarized case, if the primary noise sources scale independently of the signal and/or with Poisson counting statistics. The form of Equation (23) highlights that the photometric noise scales as expected from individual samples being averaged together, shrinking by a factor of $\sqrt{3}$ when the polarizer triplet exposures are merged.

Turning to pB, the derivative of Equation (7) is just

$$\frac{\partial p\bar{B}}{\partial \bar{B}_i} = -\frac{4}{3} C_i. \tag{24}$$

The quadrature sum is

$$\Delta pB = \frac{4}{3} \sqrt{\sum_i C_i^2 \Delta B_i^2} = \frac{4}{3} \sqrt{\frac{3}{2} (\Delta_c B)^2 + B_0 \sum_i (C_i^2 B_i)}. \tag{25}$$

Substituting with Equation (11) to eliminate the B_i term yields

$$\Delta pB =$$
$$\frac{4}{3} \sqrt{\frac{3}{2} (\Delta_c B)^2 + \frac{3}{2} \frac{B_0 B}{2} - \frac{B_0}{2} \left(pB \sum_i C_i^3 + pB' \sum_i C_i^2 S_i \right)} \tag{26}$$

where the summation terms oscillate in $\theta - \alpha$, with individual amplitude $3/4$ and frequency 6 per full circle in θ. It is useful to bound the right-hand-side of Equation (26). The maximum value of the square root occurs when the oscillating term has its minimum (most negative) possible value. That occurs at the extremal value of pB and/or pB', such that $pB^2 + pB'^2 = B^2$. Setting $pB = B$ and $pB' = 0$, and selecting the minimum value of the C_i^3 sum, yields

$$\Delta pB \leqslant \frac{2\sqrt{2}}{\sqrt{3}} \sqrt{(\Delta_c B)^2 + \frac{3}{4} B_0 B}, \tag{27}$$

which can be simplified further. Adding $(\Delta_c B)^2/2$ to the interior is allowed in the inequality, and yields a much simpler expression at the cost of slightly expanding the bound:

$$\Delta pB \leqslant 2\sqrt{(\Delta_c B)^2 + B_0 B/2} = \sqrt{3}\, \Delta B. \tag{28}$$

Systems that have nonzero values of pB' have the same upper bound for ΔpB, because when the total relative polarization is maximized, mixing pB and pB' is equivalent to rotating the polarizers (changing θ), which does not affect the minimization of the summation terms across $\theta - \alpha$.

The upper bound for pB' clearly must be the same as for pB, because the two quantities are related by a rotation—and neither θ nor α appears in Equation (28). We therefore immediately write

$$\Delta pB' \leqslant \sqrt{3}\ \Delta B. \tag{29}$$

In sum: although the photometric noise level in the derived value of pB (and, by extension, other related quantities pB', Q, and U) from Equation (7) varies with overall polarizer angle θ, a simple upper bound exists that is independent of θ and (equivalently) position angle α. Photometry in polarized brightness parameters is worse than the unpolarized overall photometry, by a factor of up to $\sqrt{3}$.

3.1.2. Polarizer Misalignments

Instrument polarizers are mechanical devices and subject to alignment tolerance. The triplet (M, Z, P) system (introduced between Equation (6) and Equations (7) and (9)) relies on a trigonometric identity to simplify the weighted average in Equation (6). Errors in polarizer angle for a particular exposure translate directly to errors in B and pB independent of photometric noise. Even assuming either perfect alignment or proper angular calibration (using, e.g., Equation (6) or perturbation analysis on Equation (7)), individual polarized intensity images will be polarized at an angle that differs slightly from nominal, due to noise in the alignment process. Following the same methodology as in Section 3.1.1, we characterize polarimetric response to this type of noise by treating noise-associated error in polarizer angle as a random variable. We then propagate the noise from the foundational equations to Equations (7), (9), and (10) by partially differentiating.

We start by characterizing B_θ's θ-dependence. From Equation (11),

$$\frac{\partial B_i}{\partial \theta_i} = S_i\, pB - C_i\, pB' \tag{30}$$

and, from Equation (9) (and making use of the same identity as in Equation (7)),

$$\frac{\partial \overline{B}}{\partial \theta_i} = \frac{2}{3}\{S_i\, pB - C_i\, pB'\}. \tag{31}$$

Treating three $\Delta\theta_i$'s in quadrature (and making use of the same identity as in Equation (26)),

$$\Delta B = \frac{\sqrt{2}}{\sqrt{3}} \sqrt{pB^2 + pB'^2}\, \Delta\theta. \tag{32}$$

Equation (32) describes a noise term in B whose magnitude is dependent on the total degree of linear polarization regardless of direction.

Applying the same process to pB, we have from Equations (6) and (30)

$$\frac{\partial p\overline{B}}{\partial \theta_i} = \frac{1}{\sum_k C_k^2}\left\{\sum_j (B - 2B_j)(-2S_i\delta_{ij})\right\}$$
$$+ \frac{1}{\sum_k C_k^2}\left\{\sum_j (2/3)(S_j\, pB - C_j\, pB')C_j\right\}$$
$$+ \frac{1}{\sum_k C_k^2}\left\{\sum_j (-2(S_j\, pB - C_j\, pB')\delta_{ij}C_j)\right\}$$
$$- \frac{2C_i(-2S_i)}{\left[\sum_k C_k^2\right]^2}\sum_j \{(B - 2B_j)C_j\}, \tag{33}$$

where δ_{ij} is the Kronecker δ. Merging terms, and where possible eliminating those terms which sum to zero, simplifies Equation (33) considerably and yields

$$\frac{\partial p\overline{B}}{\partial \theta_i} = \frac{2}{3}\{-2(B - 2B_i)S_i$$
$$- 2(S_i\, pB - C_i\, pB')C_i + 4C_i S_i\, pB\}. \tag{34}$$

Solving Equation (11) for the quantity $B - 2B_\theta$, and substituting in to simplify Equation (34) further,

$$\frac{\partial p\overline{B}}{\partial \theta_i} = \frac{2}{3}\{-2(C_i\, pB + S_i\, pB')S_i$$
$$- 2(S_i\, pB - C_i\, pB')C_i + 4C_i S_i\, pB\}, \tag{35}$$

or, gathering terms and applying the double-angle identity,

$$\frac{\partial p\overline{B}}{\partial \theta_i} = \frac{4}{3}\cos[4(\theta_i - \alpha)]pB'. \tag{36}$$

Equation (36) describes a noise coupling term in $p\overline{B}$ that is proportional to pB'. Therefore, because pB' is negligible in the bright inner corona, small errors in polarizer angle have negligible effect on the pB calculations in that field. This surprising result helps explain why triplet polarization has performed well in historical coronagraph data: in the inner few apparent solar radii of the corona, such systems are insensitive to small polarizer misalignments. The corresponding error term is as curiously silent as a dog that does nothing in the night (Doyle 1892).

Applying three $\Delta\theta_i$'s in quadrature yields

$$\Delta pB = \frac{2\sqrt{2}}{\sqrt{3}}\, pB'\, \Delta\theta. \tag{37}$$

Arguing from symmetry, we can also immediately write

$$\Delta pB' = \frac{2\sqrt{2}}{\sqrt{3}}\, pB\, \Delta\theta. \tag{38}$$

In sum: polarizer misalignment in principle produces photometric error in derived polarization parameters. The resulting error in unpolarized brightness B depends on total polarization and not, to first approximation order, on its direction. The corresponding error in pB calculation depends only on the cross mode polarization pB', and vice versa.

3.1.3. Polarizer Effectiveness

The analysis leading to Equations (7), (9), and (10) assumed perfect polarizers. In practice, real polarizers are not perfectly effective and instead have a finite extinction coefficient. A real instrument with physical polarizers will produce observed polarizer brightnesses $\bar{B}_\theta$ with

$$\bar{B}_\theta = B_\theta + \epsilon B, \qquad (39)$$

where ϵ is a small leakage coefficient (and of course an overall efficiency factor is removed via photometric calibration). If ϵ is known, it can be calibrated out. Equation (39) propagates into Equation (7) as

$$pB = -\frac{4}{3}\sum_i [(\bar{B}_i - \epsilon_i B)C_i]. \qquad (40)$$

In the case where all the ϵ_i terms are equal, Equation (40) reduces to Equation (7); i.e., finite polarizer extinction effects do not affect pB measurement or, by symmetry, pB' measurement, provided that they are constant across polarizers.

Likewise, substituting $B = \bar{B}_i - \epsilon_i B$ into Equation (9), we obtain

$$B = \frac{2}{3}\frac{\sum_i \bar{B}_i}{\left(1 + \frac{2}{3}\sum_i \epsilon_i\right)}, \qquad (41)$$

so that, if all ϵ_i terms are equal, then the calculated B_i value must be scaled by a factor of $1 - 2\epsilon$, to first approximation order, relative to the naïve perfect-polarizer formula in Equation (9).

In sum: the polarizer extinction coefficient ϵ^{-1} does not affect inferred values of pB or pB', provided that it is constant across polarizer positions. The extinction coefficient does affect the inferred value of B, which can be corrected provided that ϵ is known. As an example, polarizers with $\epsilon^{-1} = 200$ would incur a 1% error in the ratio pB/B from this source alone, if not corrected using Equation (41).

4. Virtual Polarizer Triplets

So far we have established the theory of measuring the (B, pB, pB') coronal polarization parameters or, equivalently, the (I, Q, U) Stokes parameters, using polarizer triplets. But the triplet formulation is useful not only as a means of measurement but also as a means to represent the linear polarization state of light. A "virtual polarizer triplet" formulation represents light as three brightness parameters through three ideal polarizers separated by $\pi/3$ radians (60°) each: the (M, Z, P) representation.

In the context of coronal imaging, virtual polarizer triplets have two distinct advantages over the Stokes representation. First, the virtual triplet is a symmetric representation: the three brightness channels all have similar properties and none is treated preferentially, unlike the Stokes and pB systems in which Stokes I (or B) is treated differently from the other parameters. Second, each parameter in the virtual triplet representation is positive-definite; this is important in the context of coronal measurements, because it improves background subtraction when the background itself is polarized.

Background subtraction for both coronagraphs and heliospheric imagers requires accumulating and modeling a "minimum background" with varying degrees of sophistication depending on field of view (e.g., Brueckner et al. 1995; Howard et al. 2008). For measurements close to the Sun, the pB' component is negligible and the background is nearly unpolarized (e.g., Wlérick & Axtell 1957). At solar elongations of a few degrees, the polarization of the F corona becomes significant (Weinberg & Hahn 1980) and its polarization must be treated differently. At solar elongations of 10° or more, the starfield itself is an important source of background light and must be eliminated independently (DeForest et al. 2011). Adding insult to injury, the starfield is itself slightly linearly polarized by as much as a few percent by the interstellar medium (e.g., Mignani et al. 2019). The positive-definite nature of virtual polarizer images allows existing background estimation methods, which apply to unpolarized radiance, to be used on each of the three polarizer channels independently. This allows the use of existing techniques for removal of these background sources and instrument stray light independently in each polarizer channel, to preserve the polarization as well as the overall brightness of the background signal (DeForest et al. 2017). Each virtual polarizer channel is itself "just" a radiance channel containing a fixed subset of the overall brightness observed by the instrument, and existing techniques for finding a running-minimum brightness apply.

Because the starfield and the F corona are fixed in different coordinate systems, removing them requires operating not only in different pixel coordinates (DeForest et al. 2011) but also in different polarization coordinates. In particular, a linear polarization signal from a particular star will maintain a fixed direction in celestial coordinates but have variable direction of polarization in solar observing coordinates. Therefore, coronal polarization values accumulated in an instrument coordinate system must be transformed into solar coordinates to identify and remove the F corona, then into celestial coordinates to identify and remove the starfield; then back into solar coordinates for further analysis. This echoes the pixel resampling that is also necessary to eliminate those background sources.

In Section 3 we derived how to convert brightness values measured through a triplet of polarizers into either Stokes parameters (Equations (9), (12) and (13)) or (B, pB, pB') (Equations (9), (7), and (10), respectively). The inverse transform from either the Stokes or (B, pB, pB') system to a virtual polarizer triplet at angle θ is given in Equation (11). Here, we derive how to convert directly between M, Z, P virtual triplet representations with different values of θ.

Consider a polarizer at angle ϕ. Substituting Equations (7), (9), and (10) into Equation (11) gives

$$B_\phi = \frac{1}{2}\left\{\frac{2}{3}\left[\sum_i B_i\right] + \cos[2(\phi - \alpha)]\right.$$
$$\left. \times \left[\frac{4}{3}\sum_i (B_i C_i)\right] + \sin[2(\phi - \alpha)]\left[\frac{4}{3}\sum_i (B_i S_i)\right]\right\}. \qquad (42)$$

Gathering terms across the finite sums gives

$$B_\phi = \frac{1}{3}\sum_i \{B_i + 2B_i (\cos[2(\phi - \alpha)]C_i + \sin[2(\phi - \alpha)]S_i)\}, \qquad (43)$$
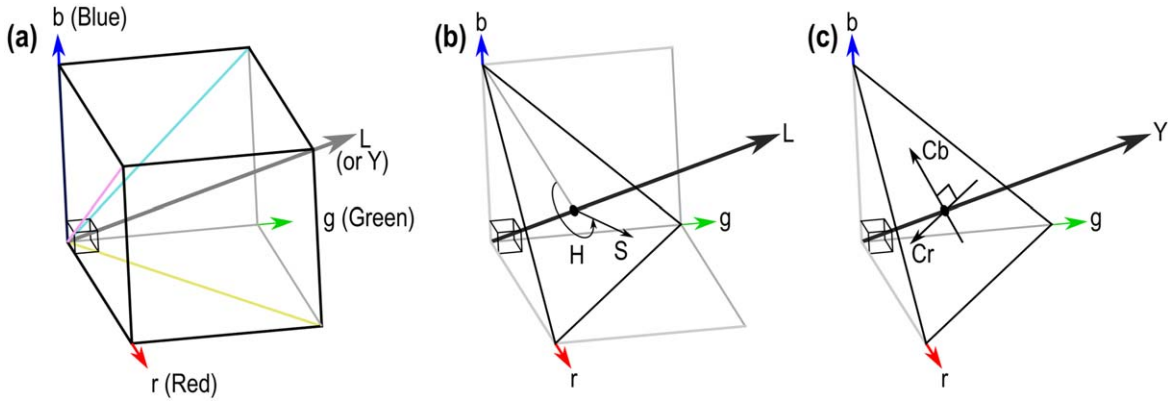
Figure 2. Systems for representing color parameterize a 3-space that is analogous to the 3-space needed to represent linear polarization. (a) (r, g, b) uses conventional Cartesian coordinates to represent three separate radiances in different primary colors. (b) (H, S, L) and (H, C, L) use conical and cylindrical coordinates, respectively, around a "white line" balancing r, g, and b, with L and C having units of radiance and $S \equiv C/L$. (c) (Y, Cb, Cr) uses Cartesian coordinates rotated to align with the white line.

which simplifies to

$$B_\phi = \frac{1}{3}\sum_i \{B_i(1 + 2\cos[2(\phi - \theta_i)])\}, \qquad (44)$$

and thus to

$$B_\phi = \frac{1}{3}\sum_{i \in \{M,Z,P\}} B_i[4(\cos[\phi - \theta_i])^2 - 1]. \qquad (45)$$

Equation (45) yields the predicted brightness through a polarizer at angle ϕ, given the brightness through an (M, Z, P) triplet of three linear polarizers at angle θ, i.e., a set of three linear polarizers at $\theta - \pi/3$, θ, and $\theta + \pi/3$.

Important properties of Equation (45) include: (a) B_ϕ is by construction nonnegative for physical values of the B_i's; (b) setting $\phi = \theta_i$ for any of the i's recovers the relation $B_\phi = B_i$; and (c) the equation is numerically stable, with no potential poles or singularities.

Applying Equation (45) to create predicted brightnesses for an (M, Z, P) triplet of polarizers at $\phi - \pi/3$, ϕ, and $\phi + \pi/3$ constitutes a change of basis, fully describing the polarization state not via direct brightnesses transmitted through a triplet of physical polarizers but via predicted brightnesses through a triplet of ideal "virtual polarizers" at an arbitrary angle ϕ. Provided only that both θ and ϕ are known, the transformation via Equation (45) preserves the full polarization state recorded by the original triplet.

5. Representations of Polarization and of Color

There is a strong analogy between representations of color and representations of linear polarization.

The normal human visual system has three separate color channels at long, medium, and short wavelengths, conventionally labeled "red," "green," and "blue," comprising a 3D space (e.g., Young 1802; Maxwell 1857; Feynman et al. 1963). The components are conventionally labeled (r, g, b), with each representing radiance of light with a particular spectral characteristic (a "primary color" of the system, which forms a basis vector for the 3-space). In practice, a large number of slightly different (r, g, b) systems exist, using slightly different primary colors. All such spaces share the property of being positive-definite, like the radiance values discussed in Section 3; this forms a positive-definite "gamut" that

encompasses a subset of all possible colors (Figure 2(a)). Representing colors outside the gamut would require negative brightnesses of the primary colors, which is not physically possible. Because of peculiarities of the human eye, no three primary color vectors can both have positive-definite spectra (which may be reproduced in the laboratory) and also encompass all humanly perceptible colors. The CIE 1931 (X, Y, Z) color space (Smith & Guild 1931) is a standard (r, g, b) system that uses nonphysical primary colors with negative spectral intensities at some wavelengths to provide a positive-definite gamut that encompasses all of human vision, at the cost of requiring conversion to a physical (r, g, b) system before the color can be rendered for viewing. (Note that the Z in (X, Y, Z) is distinct from the Z in (M, Z, P): the former represents a blue-like fictional primary color, while the latter represents zero polarizer offset from a reference angle θ.)

The (r, g, b) systems are far from the only representations of color space. Two other large classes are equally important.

Hue systems are based on the Munsell (1912) color wheel, which parameterizes the space as hue, "chroma," and "luminance" (H, C, L). These systems are based around a cylindrical projection of (r, g, b) space. Luminance is a radiance of white light (distance from the origin along a defined "white line" in colorimetric space, so that r, g, and b have a given fixed ratio); chroma is a radial distance in the plane perpendicular to the white line at particular radiance (the "chroma plane"); and hue gives the angle at which the radius is to be drawn in that plane (Figure 2(b)). A more common variant of the (H, C, L) system is (H, S, L); this system replaces C (chroma) with a relative value S ("saturation") defined via $S \equiv C/L$, and also replaces L (luminance) with a closely related quantity "lightness".

"Opponent" color systems work similarly to (H, C, L) systems: they represent color with luminance (usually Y from the (X, Y, Z) system) and 2D signed chroma values in the chroma plane. The (Y, Cb, Cr) system (International Telecommunications Union 2017) has an unsigned luminance signal indicating distance from the origin along the white line, and two signed "chrominance" signals (with units of radiance) that describe location in the perpendicular plane (Figure 2(c)). Here, Y represents luminance and is normally a linear combination of the (r, g, b) signals: $Y \equiv K_r r + K_g g + K_b b$, with $\sum_i K_i^2 = 1$. For convenience in this cursory treatment, we ignore this scaling, effectively setting $Y = L$ and $K_i = 1/\sqrt{3}$ for each K_i. The

(Y, Cb, Cr) and related color-opponent systems are important both for video coding and because they describe well the perceptual aspects of the human visual system, as can be verified by direct visual experiment (Churchland 2005).

Converting from (r, g, b) to (Y, Cb, Cr) is a simple linear transformation. With $\hat{Y} \cdot \hat{r} = \hat{Y} \cdot \hat{g} = \hat{Y} \cdot \hat{b}$ by construction, the realization that the chroma-plane-projected $(\hat{r}', \hat{g}', \hat{b}')$ vectors are separated by $\pi/3$, and direct evaluation of $\cos(\pi/3)$ and $\sin(\pi/3)$, the coefficients may be written down by simple inspection:

$$Y = \frac{2}{3}[r + g + b], \tag{46}$$

$$Cb = \frac{1}{\sqrt{3}}[2b - r - g], \text{ and} \tag{47}$$

$$Cr = \frac{2}{\sqrt{3}}(r - g). \tag{48}$$

The Cb and Cr formulae describe perpendicular vectors in the chroma plane. The Cb formula arises because of the symmetry of the triangle formed by the projected $(\hat{r}', \hat{g}', \hat{b}')$ directions in the chroma plane and the fact that $\hat{Cb}$ is parallel to $\hat{b}'$. The Cr formula is simpler because $\hat{Cr}$ is parallel to the $\hat{g}' - \hat{r}'$ line and perpendicular to $\hat{b}'$.

Equations (46), (47), and (48) echo Equations (9), (12), and (13) respectively, establishing the analogy between (r, g, b) colors and polarizer triplet brightnesses—and, similarly, between (Y, Cb, Cr) colors and the linear Stokes parameters.

Moving to the (H, S, L) system, measuring the hue angle relative to $\hat{b}'$ immediately gives

$$H = \arctan[Cr/Cb], \tag{49}$$

where the four-quadrant arctan is implied, and

$$S = \frac{\sqrt{Cr^2 + Cb^2}}{Y}. \tag{50}$$

Again, this echoes directly the structure of Equations (15) and (16), converting from the Stokes formulation to the (B, θ, p) system, with Y, H, and S corresponding to B, $2\theta'$, and p respectively (where θ' has the appropriate reference angle subtracted for either the (I, Q, U) or (B, pB, pB') system).

Two useful insights come immediately from the connection between polarization and color spaces. The first is an understanding of why polarizer triplets are convenient and numerically stable representations of polarization space: they are simply 3-vectors in the space, forming an orthonormal basis. Polarizer triplet (or virtual polarizer triplet) brightness parameters have a higher degree of mutual symmetry than do Stokes parameters (which are themselves a different orthonormal basis of the same space), but as orthornormal bases they are easily analyzed, manipulated, and interconverted.

The second useful insight is the notion of a "physical gamut"—the range of values that are both representable and not physically impossible, within a given representation space. Because radiances of light cannot be negative, and the spectra of the human eye's photosensitive pigments (treated as very-high-dimensional vectors) are not perpendicular, no physically realizable primary colors can represent all of human color in a tricolor system. The specific (X, Y, Z) system of (r, g, b) primary colors (Smith & Guild 1931) uses impossible (nonphysical) spectra to achieve a gamut that can represent any possible color of light, at a cost of requiring conversion to a specific physical colorimetric system before color can be rendered in the physical world.

A peculiarity of (X, Y, Z) is that it can also represent physically impossible colors that cannot exist at all, even in principle, because they cannot be rendered with any positive-definite spectrum of light. This is also the case for (M, Z, P) systems for representing polarization: some of the possible vectors yield values of pB and pB' (or, equivalently, Stokes Q and U) that are outside the Stokes inequality $B^2 \geqslant pB^2 + pB'^2$, which determines physically possible polarization states. In the (X, Y, Z) system, the physically realizable colors occupy an irregularly shaped locus in the chroma plane, driven by the specific absorption spectra in the human eye. In an (M, Z, P) system, the physically realizable polarizations (that satisfy the Stokes inequality) form a circle in the "polarization plane" described by (pB, pB') or (Q, U); the circle is a cross section of the Poincaré sphere (Born & Wolf 1999), neglecting the third Stokes perturbation parameter V.

Happily, the circle is inscribed in the triangle formed by the (M, Z, P) gamut on the polarization plane in polarimetric space, as can be verified by direct substitution into Equation (11). This triangle is exactly analogous to the triangle in the chroma plane formed by the (r, g, b) gamut, which may be seen in Figures 2(b) and (c).

The presence of the "Poincaré circle" physical gamut inside the triangular (M, Z, P) gamut ensures that all valid polarization states may be represented by any suitable (M, Z, P) triplet of polarizers (as in Equation (45)), because the circle maps to itself under rotations about the central point.

Many impossible polarizations (which do not satisfy the Stokes inequality and are therefore outside the Poincaré circle) may be represented with a particular polarizer triplet. Substituting such triplet values into Equation (45) may yield negative polarizer radiances in the new system. As a trivial example, a point with $B_{\theta,M} = B_{\theta,P} = 0$ and $B_{\theta,Z} = 1$ yields negative values of B_ϕ for nearly all values of $\phi - \theta$, because no physically realizable polarization state can produce that combination of radiances through an ideal linear polarizer triplet. Contrariwise, all physically realizable states exist within the Poincaré circle, which is inscribed in all possible polarizer triplet gamuts on the polarization plane, and therefore those states all yield positive values from Equation (45) regardless of the value of $\phi - \theta$.

In sum: the principal systems of representing linear polarization are mathematically analogous to the principal systems of representing color. This yields both intuition, via the connection to (r, g, b) color systems, and insights into why the polarizer triplet system works well for representing linear polarization of light.

6. Conclusions

Linear polarization is an important measurement of the solar corona and heliosphere. In the solar case, the Stokes parameters (I, Q, U), which are defined in the instrument frame of reference, are not the most convenient measure of polarization; instead, because of the peculiarities of polarization in the visible solar corona, a large body of past and current literature treats the polarized brightness as a sort of "virtual Stokes parameter" oriented relative to the image-plane solar radial direction rather than in a particular instrument direction, with its Stokes complement pB' generally ignored. Building on that

practical and implicit treatment, we have presented the derivation of the Stokes-equivalent B, pB, and pB' parameters directly from a triplet of brightness values in three polarizers. While the three-polarizer approach to measuring coronal polarization was described (in Russian) by Fesenkov ([1935](#)) and more briefly (in English) by Öhman ([1947](#)) and Billings ([1966](#)), and is now commonly used in many instruments, the derivation has generally used an asymmetric transition through the Stokes parameters and/or been given cursory treatment.

Instruments making use of a polarizer triplet are subject to particular uncertainties in measurement that are peculiar to the polarizer triplet system. A literature search found no complete analytic treatment of these in-principle knowable noise sources. Accordingly, we have presented the effects of three major error or noise sources in three-polarizer instruments on polarimetry derived using the formulae presented here. These error sources are: per-channel photometric error; polarizer orientation error; and finite polarizer extinction coefficient. The most surprising result is that polarizer orientation error does not affect the pB measurement to first approximation order, in the inner few solar radii of the solar corona where total polarization is in the tangential (pB) direction. Our noise results supply first-order derivations of the contributions from these major noise sources to uncertainty in the calculated quantities B, pB, and pB', for uncorrelated, approximately Gaussian noise in the measured radiances. Readers are cautioned that specific definitions of derived parameters can affect noise terms in subtle ways, if those quantities are not linearly related to the source measurements. For example, even "well behaved" zero-mean, Gaussian-distributed photometric noise (such as we considered here) produces a net offset (nonzero mean) perturbation in derived values for the total polarized brightness, $^{\circ}pB \equiv (Q^2+U^2)^{1/2} = (p)(B)$, due to geometrical effects in parameter space (Inhester et al. [2021](#)).

The three-polarizer representation of polarization is symmetric and readily transformed to different orientations. Using "virtual polarizer triplets," to represent polarization data symmetrically in multiple frames, conveniently maintains the positive-definite and symmetric properties of polarizer triplet measurements without corresponding physical polarizers. The mathematical transformation between different three-polarizer systems is readily evaluated and numerically stable, making virtual polarizer triplet analysis a useful approach for converting polarization data between different coordinate systems.

Possible applications for a virtual polarizer triplet representation include regularizing polarimetry from a coronagraph or heliospheric imager that orbits the Sun or Earth, and subtracting multiple types of data background that are polarized in different coordinate systems relative to the instrument. Three such overlapping backgrounds are potentially polarized instrument stray light (fixed in the instrument frame), wide-field F corona (fixed in the solar frame), and the starfield (fixed in the celestial frame).

There is a direct mathematical analogy between representations of linear polarization and representations of visual color; this analogy may help guide intuition for the analytic derivations presented here and potentially other applications of polarization space. The (M, Z, P), (B, pB, pB') and Stokes, and (B, θ, p) systems of representing linear polarization are seen to be direct analogs of the (r, g, b), (Y, Cb, Cr), and (H, S, L) systems for representing color. With this understanding, it becomes clear why the polarizer triplet system works well for

representing and manipulating polarization values. The triplet brightness values are immediately seen to form an orthonormal basis of the polarization space; and physically allowable polarization states are seen to be representable independent of reference angle, because of the circular geometry of the Poincaré sphere.

Appendix
Definitions of pB

Historically, the fact that the corona is tangentially polarized has led to ambiguity in the term pB, which depending on context is used to refer either to total polarization or to only a certain component of polarization. In the former case, authors define and use a quantity like $^{\circ}pB \equiv (Q^2 + U^2)^{1/2}$ (where Q and U are the relevant Stokes parameters and Stokes V is neglected). $^{\circ}pB$ is thus the total polarized brightness regardless of direction, and is analogous to C in the (H, C, L) color system in Section [5](#). In the latter case, authors define and use a quantity like $^{\perp}pB \equiv B_T - B_R$, i.e., the difference between the radiance observed through a tangentially aligned linear polarizer and a radially aligned one. $^{\perp}pB$ is effectively a variant on the Stokes parameter Q, oriented radially in a solar image plane (Figures [1](#)(a) and (c)).

The distinction between $^{\circ}pB$ and $^{\perp}pB$ is nearly moot in lower coronal studies, where observed light happens to be polarized perpendicular to the focal-plane solar radial direction, though $^{\circ}pB$ responds counterintuitively to photometric noise (Inhester et al. [2021](#)). But the two quantities generalize differently in cases where the overall polarization does not happen to be tangential—for example, in wide-field coronagraphs or polarizing heliospheric imagers, where noncoronal polarized light sources are significant sources of background radiance. In addition to instrumental stray light, two such sources are the zodiacal light (Leinert et al. [1981](#)) and the starfield itself (Heiles [2000](#)).

Use of the $^{\circ}pB$ formalism is widespread in the coronal literature. Examples include Öhman ([1947](#)) and Billings ([1966](#)), who define I_p similarly to our $^{\circ}pB$. Munro & Jackson ([1977](#)) used $^{\circ}pB$ in their analysis of the corona, apparently to avoid having to deal with angle explicitly (based on their Equation ([3](#)), which treats Thomson scattering). More recently, the SOHO/UVCS (Kohl et al. [1995](#)), SOHO/LASCO (Brueckner et al. [1995](#)), and STEREO/SECCHI (Howard et al. [2008](#)) analysis pipelines calculated $^{\circ}pB$ explicitly (e.g., Ofman et al. [2000](#); Dere et al. [2005](#)); and sources as recent as Vorobiev & Ninkov ([2014](#)) and Reginald et al. ([2017](#)) use the formalism in describing new polarimetric techniques using multiplexed single-frame polarimetric detectors.

The $^{\perp}pB$ formalism is equally widespread through the coronal literature, and seems to extend even earlier than $^{\circ}pB$. Minnaert ([1930](#)), in his seminal work on coronal polarimetry, follows Young ([1911](#)) in defining the quantity $p \equiv (J_t - J_r)/(J_t + J_r + 2A)$, in which p is relative polarization, J_t and J_r are tangentially and radially polarized elements of the visual corona, and A is an unpolarized background brightness. We can

DeForest, Seaton, & West

immediately recognize that the quantity $J_t + J_r + 2A$ is more commonly abbreviated B, and that Minnaert's $p(J_t + J_r + 2A)$ is an expression for $^\perp pB$. The HAO K coronameter (Altschuler & Perry 1972) was specifically built to exploit the tangential direction of coronal polarization, and $^\perp pB$ appears explicitly (as pB) in their analysis. Additional important references using $^\perp pB$ span six decades and include Saito (1965), Koomen et al. (1975), Crifo et al. (1983), Hayes et al. (2001), Moran & Davila (2004), Howard & Tappin (2009), de Koning & Pizzo (2011), DeForest et al. (2013, 2017), and Dai et al. (2014). All of these sources define a $^\perp pB$ and refer to it as "polarized brightness"; most refer to the quantity as pB although some use I_p instead (note that I_p is used in these sources as a synonym for $^\perp pB$ and in other sources, mentioned above, as a synonym for $^\circ pB$).

The distinction between $^\circ pB$ and $^\perp pB$ has been so blurred that some authors might even use both in the same paper, without acknowledgement of the distinction. For example, both Guhathakurta et al. (1999) and Frazin et al. (2012) compare pB values across different instruments, some of which generate $^\circ pB$ data products and some of which generate $^\perp pB$ data products.

The polarized brightness parameter pB is well entrenched in the literature, and the two meanings $^\circ pB$ and $^\perp pB$ are close enough to not differ greatly in the inner corona. However, in wide-field coronagraphs and polarizing heliospheric imagers, other polarized light sources come into play. In these contexts the two parameters differ greatly in meaning; past muddiness requires more clarity from present and future authors, who ought to define pB explicitly (as many do already) wherever it is used.

ORCID iDs

Craig E. DeForest ⦿ https://orcid.org/0000-0002-7164-2786
Daniel B. Seaton ⦿ https://orcid.org/0000-0002-0494-2025
Matthew J. West ⦿ https://orcid.org/0000-0002-0631-2393

References

Altschuler, M. D., & Perry, R. M. 1972, SoPh, 23, 410
Arago, F. 1843, Ann. Philos. Discov. Month Report Progr. Sci. Art, 1, 209
Billings, D. E. 1966, A Guide to the Solar Corona (New York: Academic)
Born, M., & Wolf, E. 1999, Principles of Optics (7th ed.; Cambridge: Cambridge Univ. Press), 31
Brueckner, G. E., Howard, R. A., Koomen, M. J., et al. 1995, SoPh, 162, 357
Churchland, P. 2005, Philos. Psychol., 18, 527
Crifo, F., Picat, J. P., & Cailloux, M. 1983, SoPh, 83, 143
Dai, X., Wang, H., Huang, X., Du, Z., & He, H. 2014, ApJ, 780, 141
de Koning, C. A., & Pizzo, V. J. 2011, SpWea, 9, 03001
DeForest, C. E., de Koning, C. A., & Elliott, H. A. 2017, ApJ, 850, 130
DeForest, C. E., Howard, T. A., & Tappin, S. J. 2011, ApJ, 738, 103
DeForest, C. E., Howard, T. A., & Tappin, S. J. 2013, ApJ, 765, 44
Dere, K. P., Wang, D., & Howard, R. 2005, ApJL, 620, L119
Doyle, A. C. 1892, The Strand Mag., 4, 645
Fesenkov, V. G. 1935, Russ. Astron. J., 12, 310
Feynman, R. P., Leighton, R. B., & Sands, M. 1963, The Feynman Lectures on Physics, Vol. 1 (Pasadena, CA: California Institute of Technology), 35
Filippov, B. P., Molodensky, M. M., & Koutchmy, S. 1994, in IAU Colloq. 144, Solar Coronal Structures, ed. V. Rusin, P. Heinzel, & J.-C. Vial, 601
Frazin, R. A., Vásquez, A. M., Thompson, W. T., et al. 2012, SoPh, 280, 273
Guhathakurta, M., Fludra, A., Gibson, S. E., Biesecker, D., & Fisher, R. 1999, JGR, 104, 9801
Hayes, A. P., Vourlidas, A., & Howard, R. A. 2001, ApJ, 548, 1081
Hecht, E., & Zajac, A. 1974, Optics (Reading, MA: Addison-Wesley)
Heiles, C. 2000, AJ, 119, 923
Howard, R. A., Moses, J. D., Vourlidas, A., et al. 2008, SSRv, 136, 67
Howard, T. A., & Tappin, S. J. 2009, SSRv, 147, 31
Inhester, B., Mierla, M., Shestov, S., & Zhukov, A. N. 2021, SoPh, 296, 72
International Telecommunications Union 2017, Coding-independent Code Points for Video Signal Type Identification ITU-T H.273, http://handle.itu.int/11.1002/1000/14661
Kohl, J. L., Esser, R., Gardner, L. D., et al. 1995, SoPh, 162, 313
Koomen, M. J., Detwiler, C. R., Brueckner, G. E., Cooper, H. W., & Tousey, R. 1975, ApOpt, 14, 743
Leinert, C., Richter, I., Pitz, E., & Planck, B. 1981, A&A, 103, 177
Lyot, B. 1930, BuAst, 6, 305
Maxwell, J. C. 1857, Trans. R. Soc. Edinburgh, 21, 275
Mignani, R., Shearer, A., Słowikowska, A., & Zane, S. 2019, Astronomical Polarisation from the Infrared to Gamma Rays (Berlin: Springer)
Minnaert, M. 1930, ZAp, 1, 209
Moran, T. G., & Davila, J. M. 2004, Sci, 305, 66
Munro, R. H., & Jackson, B. V. 1977, ApJ, 213, 874
Munsell, A. H. 1912, Am. J. Psychol., 23, 236
Newkirk, G. J., Dupree, R. G., & Schmahl, E. J. 1970, SoPh, 15, 15
Ofman, L., Romoli, M., Poletto, G., Noci, G., & Kohl, J. L. 2000, ApJ, 529, 592
Öhman, Y. 1947, StoAn, 15, 2.1
Poland, A. I., & Munro, R. H. 1976, ApJ, 209, 927
Reginald, N. L., Gopalswamy, N., Yashiro, S., Gong, Q., & Guhathakurta, M. 2017, JATIS, 3, 014001
Saito, K. 1965, PASJ, 17, 1
Smith, T., & Guild, J. 1931, TrOS, 33, 73
Vorobiev, D., & Ninkov, Z. 2014, Proc. SPIE, 9143, 91435F
Weinberg, J. L., & Hahn, R. C. 1980, in IAU Symp. 90, Solid Particles in the Solar System (Dordrecht: D. Reidel), 19
Wlérick, G., & Axtell, J. 1957, ApJ, 126, 253
Young, R. K. 1911, LicOB, 205, 166
Young, T. 1802, RSPTA, 92, 12